



33

ABSTRACT

34 The ocean is the planet's largest carbon reservoir and plays a crucial role in regulating
35 atmospheric CO₂ levels, especially in the face of climate change. In coral reef
36 ecosystems, understanding the carbonate system is critical for predicting and
37 mitigating the impact of ocean acidification on these vulnerable marine ecosystems,
38 especially as atmospheric CO₂ concentrations continue to rise. This study measured
39 *p*CO₂ over space and time in Nanwan Bay, a coral reef ecosystem in southern Taiwan,
40 to identify factors that influence its variation. The results showed that mean surface
41 water *p*CO₂ values varied seasonally, with values of 393.7 (±10.8), 406.3 (±16.1),
42 399.2 (±18.6), and 366.9 (±14.5) μatm in spring, summer, fall, and winter,
43 respectively. These seasonal mean differences ($\Delta p\text{CO}_2$) relative to atmospheric *p*CO₂
44 were 7.7 (±10.8), 29.3 (±16.1), 21.2 (±18.6), and -16.1 (±14.5) μatm, respectively.
45 These findings suggest that the Nanwan Bay is a highly dynamic coral reef
46 ecosystem, exhibiting both spatial and seasonal variability in carbon exchange. The
47 carbonate system parameters of the surface water in this high-biodiversity, sub-
48 tropical marine ecosystem was influenced not only by seasonal temperature variation
49 but also by vertical mixing, intermittent upwelling, and biological effects.

50

51 **Keywords:** carbon sink, carbon source, coral reef, *p*CO₂, total alkalinity, upwelling



52

1. Introduction

53

Understanding whether the ocean acts as a carbon dioxide (CO₂) sink or source is

54

crucial in the context of climate change, as it directly affects climate regulation,

55

ecosystem health, and the effectiveness of mitigation efforts. Oceans absorb about

56

30% of human-produced CO₂ (Ipcc, 2021). If the ocean's ability to absorb CO₂

57

decreases, more CO₂ will remain in the atmosphere, exacerbating global warming.

58

CO₂ concentration in marine systems varies between region and over time (Fay et al.,

59

2021; Sitch et al., 2015; Schimel et al., 2001). For example, high-latitude temperate

60

regions and coastal seas act as sinks for atmospheric CO₂, while subtropical and

61

tropical coastal seas, estuaries, and coral reefs are generally sources (Borges et al.,

62

2005; Cai et al., 2003; Frankignoulle et al., 1998; Frankignoulle et al., 1996; Gattuso

63

et al., 1997; Gattuso et al., 1993; Ito et al., 2005; Ohde and Van Woesik, 1999; Wang

64

and Cai, 2004; Yan et al., 2011; Bates et al., 2001). The hydrological characteristics of

65

coastal waters, such as temperature, salinity, upwelling, and mixing, also exhibit

66

substantial variation, leading to differences in surface water *p*CO₂ even within the

67

same continental shelf. Furthermore, upwelling areas along the coasts of California

68

and Oman act as CO₂ sinks, whereas those along the coasts of Galicia and Oregon

69

serve as CO₂ sources (Borges and Frankignoulle, 2002; Friederich et al., 2002; Goyet

70

et al., 1998; Hales et al., 2005). Borges (2005) notes that when estuaries are included



71 in the gas exchange process, coastal seas worldwide are sources of CO₂, but they

72 become sinks when estuaries are excluded.

73 Various factors, such as temperature, tides, currents, river discharge, upwelling,
74 vertical mixing, and biological metabolism, influence CO₂ levels in coastal areas (e.g.,
75 Dai et al., 2009; Chen et al., 2024; Ibanhez et al., 2015). For instance, temperature
76 changes can directly affect the solubility of CO₂ in seawater, with higher temperatures
77 generally reduce CO₂ solubility (Dai et al., 2009). Tides and currents can enhance
78 vertical mixing, bringing CO₂-rich deep waters to the surface and increasing *p*CO₂
79 levels (Ibanhez et al., 2015; Dai et al., 2009). River discharge introduces fresh water
80 and organic matter, which can stimulate biological metabolism and further influence
81 CO₂ levels through respiration and decomposition processes (Chen et al., 2024;
82 Ibanhez et al., 2015). These factors interact and help explain why seasonal variation in
83 CO₂ levels can differ greatly across regions. For example, measurements taken at the
84 Bermuda Atlantic Time-series station in the Northwest Atlantic from 1996 to 1998
85 showed that CO₂ levels were lowest in winter and highest in summer (Takahashi et
86 al., 2002). Conversely, data collected from the Kyodo Western North Pacific Ocean
87 Time-Series station between 1998 and 2000 indicated that CO₂ levels were lower in
88 summer compared to winter (Takahashi et al., 2002).

89 Coral reef ecosystems are known for their high productivity, biomass, and

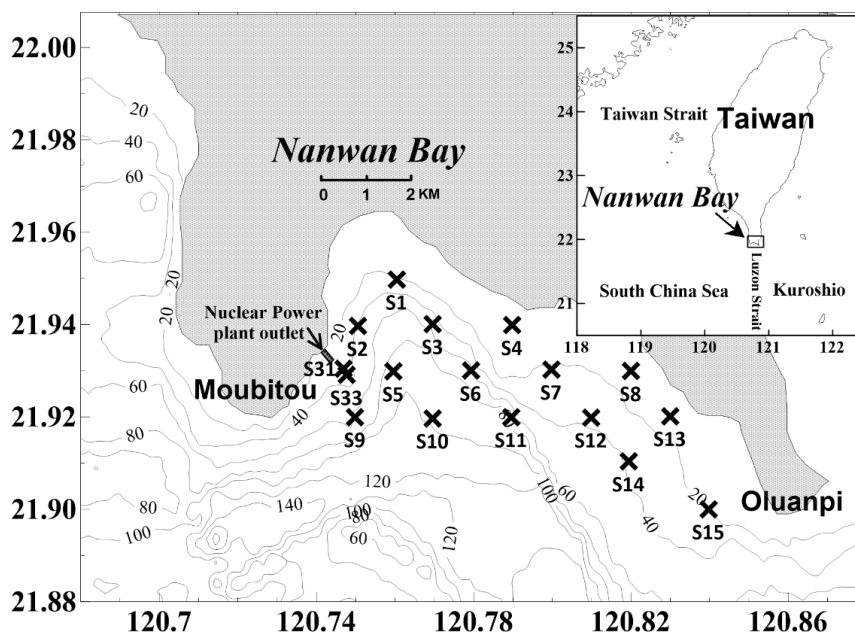


90 efficient carbonate deposition rates. However, due to their structural complexity and
91 high biodiversity, the carbon dynamics of coral reefs differ substantially from those of
92 the open ocean. Whether coral reef ecosystems function as net carbon sources (Ware
93 et al., 1992; Gattuso et al., 1993; Gattuso et al., 1999; Fagan and Mackenzie, 2007;
94 Lønborg et al., 2019; Yan et al., 2018; Watanabe and Nakamura, 2019; Frankignoulle
95 et al., 1998) or sinks (Kayanne et al., 1995; Mayer et al., 2018; Suzuki, 1998; Suzuki
96 and Kawahata, 2004) remain uncertain due to factors like the high spatial and
97 temporal variability within these ecosystems. Sedimentation rates and anthropogenic
98 influences further complicate the coral reef carbon balance. Moreover, ocean
99 acidification could reduce coral calcification rates, diminish their ability to produce
100 CO₂, thereby buffering and reducing the *p*CO₂ levels in seawater (Ries, 2011; Fabry et
101 al., 2008; Albright et al., 2016). Consequently, predicting changes in seawater carbon
102 levels in response to oceanographic anomalies remains a challenge.

103 Nanwan Bay, located at the southernmost tip of Taiwan (Fig. 1), is a semi-
104 enclosed area between Cape Moubitou and Cape Oluanpi, characterized by high-
105 biodiversity and abundant fringing coral reefs (Yang and Dai, 1980). Previous studies
106 of Nanwan Bay have noted that periodic upwelling causes the mixing of upper and
107 lower seawater layers, facilitating the transfer of nutrients from the deeper waters to
108 shallower areas (Chen et al., 2005). In most coastal upwelling regions, the ocean



109 absorbs CO₂ from the atmosphere (Hales et al., 2005), a process closely tied to the
110 increased primary production of phytoplankton in the nutrient-rich waters following
111 upwelling. Primary productivity in marine ecosystems plays a crucial role in carbon
112 cycling by driving the fixation of CO₂ (Dugdale and Wilkerson, 1989; Murray et al.,
113 1995). During periods of heightened primary productivity, the increased demand for
114 carbon can lead to greater uptake of CO₂ from seawater, potentially reducing its
115 concentration (Chen et al., 2004). Interestingly, this phenomenon has yet to be
116 explored within the coral reef ecosystem of Nanwan Bay.



117
118 **Fig. 1** Map of sampling stations (marked with “X” with the station number
119 underneath) in Nanwan Bay, Taiwan, along with contours of depth (m).

120 The difference between seawater $p\text{CO}_2$ ($p\text{CO}_2^{\text{seawater}}$) and atmospheric $p\text{CO}_2$



121 ($p\text{CO}_2^{\text{air}}$) not only serves as a metric but also determines whether a marine system
122 functions as a source or sink of carbon. In this context, a positive difference, where
123 $p\text{CO}_2^{\text{seawater}} - p\text{CO}_2^{\text{air}} > 0$, indicates a carbon source, while a negative difference
124 signifies a carbon sink. To determine whether Nanwan Bay behaves as a net carbon
125 source or sink, this study evaluates the role of hydrological conditions and their
126 potential influence on the carbonate system and CO_2 fluxes. To achieve this, we
127 conducted a comprehensive analysis of the marine carbonate system across various
128 spatial and temporal gradients.

129 **2. Methods**

130 **2.1 Study site** Nanwan Bay (Fig. 1) is flanked by the Pacific Ocean to the east,
131 the Taiwan Strait to the west, the Luzon Strait to the south, and the South China Sea
132 (SCS) to the southwest (Lee, 1999) and covers an area of $\sim 30 \text{ km}^2$ (estimated via
133 Google Earth Pro). Nanwan Bay is among the most diverse marine regions in Taiwan,
134 which led to its inclusion within Kenting National Park (Meng et al., 2008). The
135 complex seabed in Nanwan Bay encompasses diverse habitats, including: sandy
136 beaches, rocky shores, and coral reefs. This area represents the initial point of
137 interaction between the SCS waters and the warm, highly saline Kuroshio Current.
138 The water is oligotrophic, and temperatures typically range from 21 to 30°C (with
139 periodic upwelling events occurring;(Chen et al., 2005). In the course of the



140 upwelling event, the surface water of Nanwan Bay can drop by $>3^{\circ}\text{C}$, coupled with a
141 rise in nitrate concentration exceeding $2\ \mu\text{M}$, as documented by (Chen et al., 2005).
142 The bay hosts over 1,200 fish species and more than 200 species of reef-building
143 coral, making it a significant research focus area for both the reefs and the
144 anthropogenic stressor regime (Meng et al., 2007). Studies have shown that high
145 levels of nutrients and suspended solids may have contributed to the decline in coral
146 cover between 2001 and 2022 (Meng et al., 2008; Chen et al., 2022).

147 **2.2 Sampling and analysis** The study was conducted across four seasons: spring
148 (31 March 2011), summer (5 July 2011), autumn (20 October 2011), and winter (22
149 January 2013), in the area between Nanwan Bay's two capes, Moubitou and Oluanpi.
150 A total of 17 seawater sampling stations were established, including two (Sts. 31 and
151 33) located near the outlet of a nuclear power plant (Fig. 1). Temperature and salinity
152 data were collected using an Idronaut Ocean Seven 304 CTD calibrated against an
153 International Association for the Physical Sciences of the Ocean seawater standard.
154 Water samples were collected using Niskin bottles with Teflon-coated inner walls.
155 Seawater at each station was taken at two to five depths at intervals of 3 to 25 m in
156 areas shallower than 50 m; extra samples at 65, 80 and/or 100 m were taken for
157 stations with depths of 65-100 m. Please refer to Table S1 for details on the sampling
158 times and sampling depths at each station. Notably, all samples were collected



159 exclusively during daytime. Water samples were immediately analyzed for dissolved
160 oxygen (DO) content using YSI 52 and YSI 5905 BOD electrodes (factory
161 accuracy=99.9%). Other water samples were divided into different sample bottles for
162 additional analyses, including chlorophyll *a* (Chl *a*), pH, and total alkalinity (TA).
163 One 300-mL amber bottle was pre-inoculated with 0.2 mL of mercuric chloride to
164 suppress biological activity that could affect TA and other carbonate system
165 parameters.

166 For Chl *a* analysis, 1 L of seawater were was immediately filtered through GF/F
167 filter paper (Whatman, 47 mm) and stored in liquid nitrogen. The Chl *a* retained on
168 the GF/F filters was determined fluorometrically (Turner Design 10-AU-005; Parsons
169 et al., 1984).

170 Seawater pH and total TA were measured using an automated titration system
171 consisting of a Mettler-Toledo DL53 with a DG-111 electrode. Prior to measurements,
172 the electrode was calibrated using Merck standard buffer solution (NIST) at 25°C.
173 The calibration ranges for pH 4, 7, and 10 were set to fall within the range of 176±30
174 mV, 0±30 mV, and -176±30 mV, respectively (calibration slope of -56 to -59).
175 Measured pH values were expressed on the NBS scale.

176 For TA measurements, 40 g of seawater were titrated with 0.1 N HCl at 25°C.
177 Titration continued until the pH exceeded the end point (~pH 4.4) and then continued



178 until ~pH 3.0, with the potential change and titration volume recorded. The consumed
179 volume of HCl was calculated using the Gran (1952) function based on the linear
180 relationship between titration volume and pH, and TA was obtained by plotting the
181 consumed volume of HCl. The reference material for experimental quality control
182 was obtained from Professor Andrew Dickson (Scripps Institute of Oceanography,
183 USA), and the pH of the reference material was calculated by entering dissolved
184 inorganic carbon (DIC) and TA data into CO2SYS software ver. 1.02 (Lewis and
185 Wallace, 1998).

186 The pH measurement accuracy in this study was ± 0.01 units and the TA accuracy
187 was $\pm 2.7 \mu\text{mol kg}^{-1}$ (precision=0.12%). $p\text{CO}_2$ and DIC were also calculated with
188 CO2SYS from measured pH and TA. The dissociation constants of carbonic acid used
189 were the revised K_1 and K_2 values from Dickson and Millero (1987) refit from the
190 values of Mehrbach et al. (1973). Notably, the surface water $p\text{CO}_2$ was estimated
191 using the average values of samples collected at depths of 1 and 3 m at each station
192 (Table S1).

193 **2.3 Calculation of the exchange flux of CO₂ between the ocean and the**

194 **atmosphere.** The formula for calculating the exchange flux of CO₂ between the ocean
195 and the atmosphere (F_{GAS}) was as follows:

$$196 F_{\text{GAS}} = k \times K_H \times (p\text{CO}_2^{\text{seawater}} - p\text{CO}_2^{\text{air}})$$



197 where k is the gas exchange rate of CO₂ (air-sea gas transfer rate) and K_H is the
198 solubility of CO₂ gas in seawater. The air-sea gas transfer rate, k , was obtained from
199 an empirical formula based on wind speed proposed by Wanninkhof (1992): $k=0.31 \times$
200 $u^2 \times (Sc/660)^{-0.5}$, where u is wind speed 10 m above sea level (in m/s; data from the
201 Central Weather Bureau's Oceanic Center-Oluanpi buoy); and Sc (Schmidt number) is
202 a function of temperature (Wanninkhof, 1992), which can be obtained from the *in situ*
203 sea surface temperature (T) as follows:

$$204 \quad Sc = 2073.1 - 125.62 \times T + 3.6276 \times T^2 - 0.043219 \times T^3$$

205 The solubility of CO₂ gas in seawater (K_H), expressed in mol L⁻¹·atm⁻¹, was calculated
206 using the formula developed by Weiss (1974):

$$207 \quad \ln K_H = -58.0931 + 90.5069 \left(\frac{100}{T} \right) + 22.2940 \ln \left(\frac{T}{100} \right) + S \left[0.027766 - 0.025888 + \left(\frac{T}{100} \right) + 0.0050578 \left(\frac{T}{100} \right)^2 \right]$$

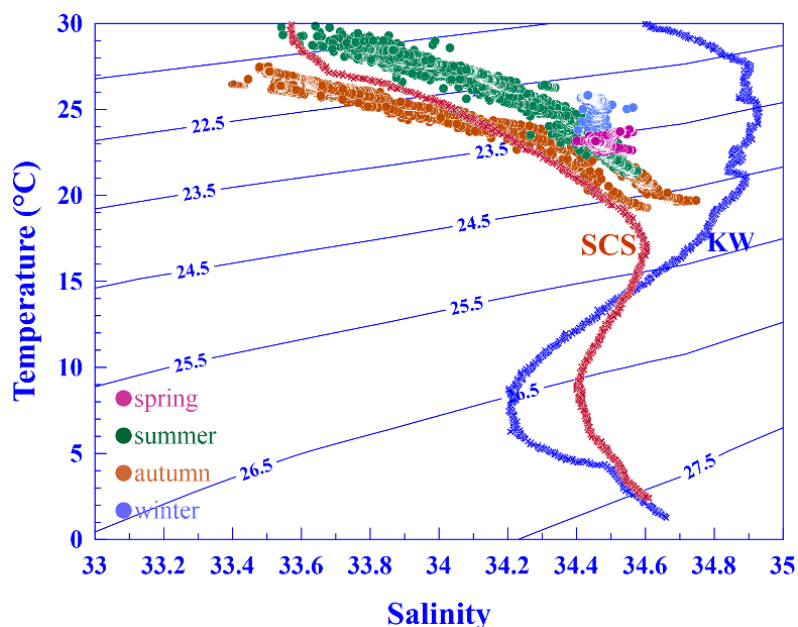
208 Since we did not directly measure $p\text{CO}_2^{\text{air}}$, we used $x\text{CO}_2$ data provided by the United
209 States National Oceanic and Atmospheric Administration (NOAA) from Dongsha
210 Island

211 ([https://gml.noaa.gov/aftp/data/trace_gases/co2/flask/surface/txt/co2_dsi_surface-](https://gml.noaa.gov/aftp/data/trace_gases/co2/flask/surface/txt/co2_dsi_surface-flask_1_ccgg_event.txt)
212 [flask_1_ccgg_event.txt](https://gml.noaa.gov/aftp/data/trace_gases/co2/flask/surface/txt/co2_dsi_surface-flask_1_ccgg_event.txt)). Dongsha Island, located at approximately 20.70°N, is a coral
213 atoll with a latitude similar to that of Nanwan Bay, and importantly, it shares the
214 characteristic of being part of a coral reef ecosystem. The dry air $x\text{CO}_2$ values were
215 corrected to 100% humidity, assuming atmospheric pressure of 1 atm, using the



216 temperature and salinity data recorded at the time of sampling. The resulting $p\text{CO}_2^{\text{air}}$
217 was 386, 377, 378, and 383 μatm on March 31, July 5, and October 18, 2011, and
218 January 22, 2013, respectively.

219 The seasonal fluxes across the bay were calculated by multiplying the mean CO_2
220 exchange flux at all stations for each season by the bay's area of $\sim 30 \text{ km}^2$.



221
222 **Fig. 2** Temperature vs. salinity (T-S) diagram at Nanwan Bay, Taiwan in spring,
223 summer, autumn, and winter. SCS = South China Sea and KW = Kuroshio
224 Waters.

225 3. Results and discussion

226 **3.1 Variation in hydrological parameters.** Both temperature and salinity varied
227 over time in Nanwan Bay (Fig. 2), with the seasonal variation likely driven by both
228 the monsoon and SCS circulation patterns as follows. The Kuroshio Current flows



229 northwards along Taiwan's east coast, with a portion of the Western Philippine Sea
230 (WPS) water following the Kuroshio and then flowing westward along the northern
231 SCS shelf (Yuan et al., 2006). Nan et al. (2015) suggested that surface salinity of 34 or
232 higher is characteristic of the Kuroshio, indicating potential inundation of the
233 Kuroshio Current into Nanwan Bay during the high-salinity spring period. During
234 summer, the southwest monsoon dominates, leading to a decrease in the Kuroshio's
235 influence; the main circulation of the Kuroshio shifts westward to the Luzon Strait,
236 limiting its intrusion into the northwestern SCS region (Liang et al., 2008). In the
237 northern SCS region, the southwest-to-northeast circulation pattern prevails during the
238 monsoon, with most seawater flowing out of the SCS through the Luzon Strait and
239 converging with the Kuroshio axis, resulting in Nanwan Bay being dominated by the
240 SCS water mass during the summer. An analysis of temperature and salinity data from
241 Nanwan Bay, the SCS, and the Kuroshio Current indicates that Nanwan Bay mainly
242 consists of the SCS water mass during summer and autumn, while during spring and
243 winter, the water masses are intermediate between the two (Fig. 2). As such, Nanwan
244 Bay is classified as a mixed water mass area, comprising both SCS and Kuroshio
245 Current water masses.

246 During the survey period, there was a clear positive correlation between pH and
247 temperature. Additionally, pH and TA exhibited significant correlations with salinity



248 **Table 1.** Correlation matrix of seawater quality variables with correlation coefficients
 249 (r) for spring, summer, autumn, and winter. Variables include temperature,
 250 salinity, dissolved oxygen (DO), DO saturation (DO%), total alkalinity (TA),
 251 dissolved inorganic carbon (DIC), and pH.

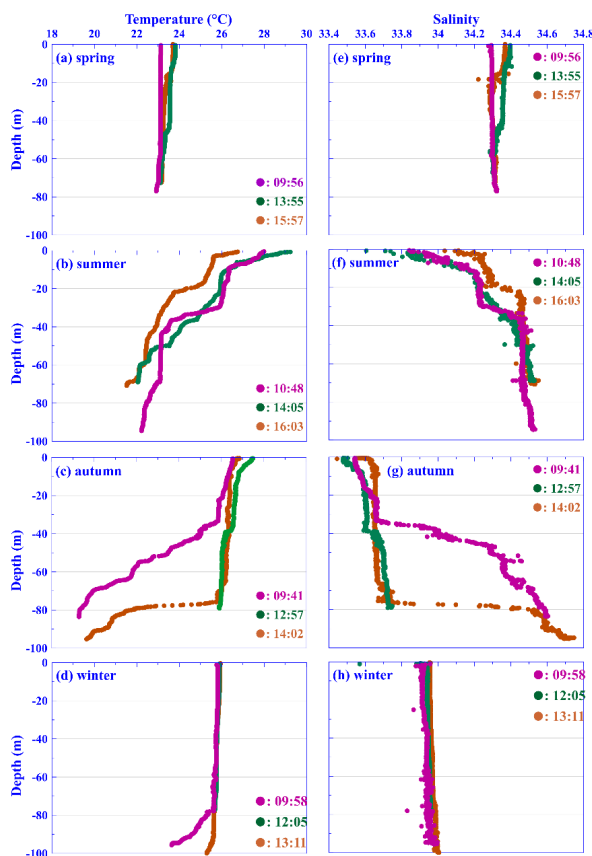
	Spring	Temperature	Salinity	DO	DO (%)	TA	DIC	pH
Salinity		0.35**						
DO		-0.23	-0.40**					
DO (%)		0.02	-0.32**	0.89**				
TA		0.04	0.03	0.19	0.11			
DIC		-0.17	-0.04	0.25*	0.11	0.92**		
pH		0.43**	0.13	-0.02	0.05	0.61**	0.27*	
$p\text{CO}_2$		-0.28*	-0.07	0.03	-0.02	-0.45**	-0.09	-0.96**
	Summer	Temperature	Salinity	DO	DO (%)	TA	DIC	pH
Salinity		-0.96**						
DO		0.65**	-0.53**					
DO (%)		0.90**	-0.81**	0.90**				
TA		-0.82**	0.81**	-0.52**	-0.72**			
DIC		-0.91**	0.84**	-0.68**	-0.87**	0.91**		
pH		0.89**	-0.79**	0.72**	0.89**	-0.72**	-0.94**	
$p\text{CO}_2$		-0.22*	0.07	-0.45**	-0.38**	0.23*	0.51**	-0.64**
	Autumn	Temperature	Salinity	DO	DO (%)	TA	DIC	pH
Salinity		-0.95**						
DO		0.88**	-0.85**					
DO (%)		0.95**	-0.93**	0.98**				
TA		-0.57**	0.56**	-0.51**	-0.55**			
DIC		-0.76**	0.75**	-0.66**	-0.72**	0.88**		
pH		0.79**	-0.77**	0.66**	0.73**	-0.43**	-0.80**	
$p\text{CO}_2$		-0.32**	0.33**	-0.22	-0.27*	0.27*	0.63**	-0.83**
	Winter	Temperature	Salinity	DO	DO (%)	TA	DIC	pH
Salinity		-0.32**						
DO		0.43**	-0.26*					
DO (%)		0.78**	-0.34**	0.70**				
TA		-0.15	0.06	-0.19	-0.17			
DIC		-0.39**	0.02	-0.34**	-0.41**	0.89**		
pH		0.59**	0.06	0.39**	0.61**	-0.12	-0.56**	
$p\text{CO}_2$		-0.34**	-0.19	-0.33**	-0.44**	0.29**	0.67**	-0.94**

255 *: $p \leq 0.05$ and **: $p \leq 0.01$.

256 during summer and autumn, but such correlations were not evident in spring and



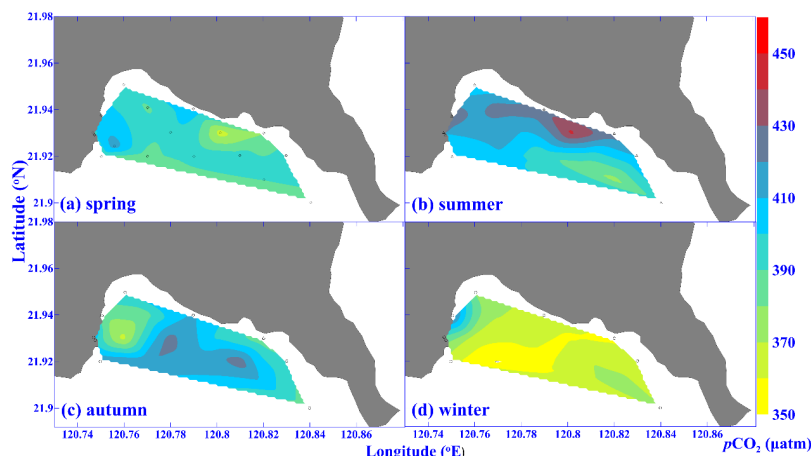
257 winter (Table 1). It is expected that TA and salinity will covary because the charge
258 differences between cations and anions in seawater change with salinity. Salinity
259 generally increases with depth and is influenced by various factors such as rainfall,
260 evaporation, and freshwater input, which can lead to changes in TA. It is worth noting
261 that the absence of a major river nearby the study sites, as well as the absence of any



262
263 **Fig. 3.** Vertical profiles of temperature and salinity at station S10 in spring (a & e,
264 respectively), summer (b & f, respectively), autumn (c & g, respectively), and
265 winter (d & h, respectively) at three sampling times (see Table S1 for details.)
266 as indicated in each panel.



267 observed rainfall events one week prior to each survey period, strongly suggests that
268 freshwater input did not play a significant role in altering TA within this study area.
269 Moreover, the absence of significant correlations among salinity, TA, and pH in spring
270 and winter implies that these relationships might be influenced by factors such as
271 intense vertical mixing or upwelling, which could disrupt the salinity, TA, and pH
272 vertical profiles. This supposition is further supported by the well-mixed profiles of
273 salinity and temperature found throughout the water column at station S10 during
274 spring and winter (Fig. 3a, d, e, & h). Additionally, seawater characterized by low
275 temperature, low pH, and high salinity observed at station S10 during the spring
276 suggests that this well-mixed pattern throughout the water column may be primarily
277 associated with upwelling during this period (Figs. 3 and S1; further details can be
278 found in the next section).



279
280 **Fig. 4.** Seasonal variation in sea surface $p\text{CO}_2$ (μatm) in Nanwan Bay, Taiwan in
281 spring (a), summer (b), autumn (c), and winter (d).

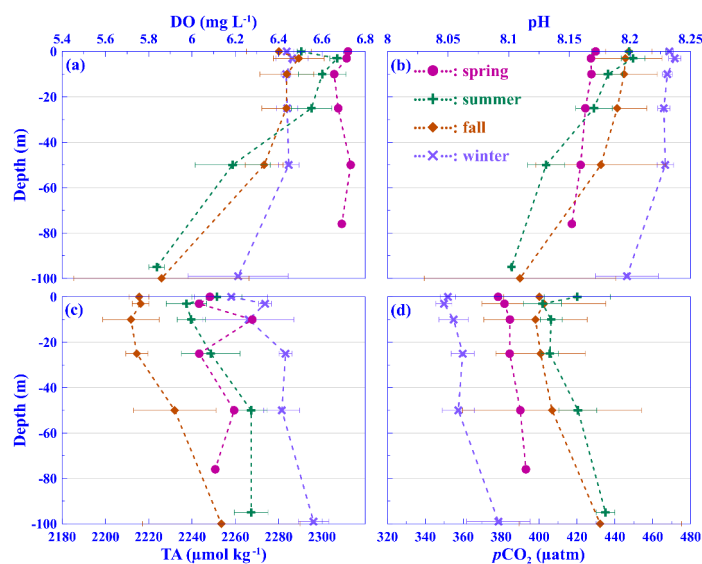


282 **3.2 Changes in surface water $p\text{CO}_2$.** Surface $p\text{CO}_2$ levels in Nanwan Bay
283 ranged from 364–422, 362–448, 350–480, and 345–427 μatm in spring, summer,
284 autumn, and winter, respectively (Fig. 4). The means values ($\pm\text{SD}$) across all stations
285 ($N = 17$) for each season were 393.2 (± 11.6), 411.4 (± 19.0), 401.7 (± 18.3), and 370
286 (± 17.3) μatm , respectively. The mean surface seawater temperatures during these
287 seasons were 23.4 (± 0.4), 28.8 (± 0.8), 27.0 (± 1.0), and 26.0 (± 0.6) $^\circ\text{C}$, respectively. In
288 the open ocean, $p\text{CO}_2$ levels are primarily influenced by temperature, horizontal
289 transport and vertical mixing, biological processes, and gas exchange (e.g., Dai et al.,
290 2009). Due to the mixing of different water masses by monsoons, tides, eddies,
291 upwelling, and other ocean currents, significant variation in temperature and salinity
292 of the water column was observed at different times at station S10 (Fig. 3) and in the
293 carbonate parameter data (Fig. 5d & S1-S4). Similarly, significant diurnal variation in
294 seawater $p\text{CO}_2$ has been reported in another coral reef ecosystem (Yan et al., 2018),
295 suggesting that more extensive temporal and spatial sampling is needed to accurately
296 capture the true dynamics of the carbonate system in coral reef environments. During
297 spring and winter, pronounced mixing was evident, as demonstrated by the straight
298 vertical profiles in temperature and salinity in Fig. 3a, d, e, and h. Conversely, in
299 summer and autumn, mixing was less apparent.

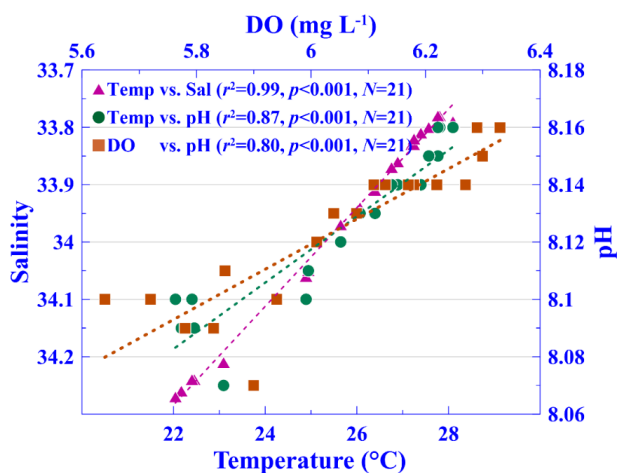
300 According to Lee et al. (1997; 1999a; 1999b), cold-water upwelling occurs with



301 tidal changes in Nanwan Bay, which increases vertical mixing. The temperature-
 302 salinity-pH-DO diagram of station S1 illustrates that throughout the entire upwelling



303
 304 **Fig. 5.** Vertical profiles of mean (\pm SD) dissolved oxygen (DO; a), pH (b), total
 305 alkalinity (TA; c), and $p\text{CO}_2$ (d) at station S10 in different seasons.



306
 307 **Fig. 6** Relationships amongst temperature and salinity or pH, as well as dissolved
 308 oxygen (DO) vs. pH, during multiple upwelling events at Station S1 (data from
 309 Tew et al., 2014).



310 event, there is an intrusion of cold, low-DO, low-pH, and high-salinity deep-sea water
311 into the nearshore regions of Nanwan Bay (Fig. 6). Seawater property profiles of S10
312 provide additional evidence of upwelling, as indicated by the presence of low
313 temperatures ($23.3\pm 0.6^{\circ}\text{C}$), low pH (8.16 ± 0.01), high salinity (34.32 ± 0.03), and
314 relatively low $p\text{CO}_2$ ($385.4\pm 5.4 \mu\text{atm}$) across the well-mixed water column in spring
315 (Figs. 3 & 5).

316 As temperature increases, CO_2 solubility decreases, causing an increase in $p\text{CO}_2$.
317 To accurately isolate and understand the specific impact of temperature variations on
318 $p\text{CO}_2$, it is crucial to normalize these factors. This approach allows for a clearer
319 distinction between temperature-induced changes and those driven by other
320 influences. Takahashi et al. (2002) proposed to evaluate the relative effects of
321 temperature and non-temperature effects on $p\text{CO}_2$ changes as follows:

$$322 \quad p\text{CO}_2 \text{ at } T_{\text{obs}} = (p\text{CO}_2)_{\text{Mean annual}} \times \exp[0.0423(T_{\text{obs}} - T_{\text{mean}})]$$

$$323 \quad p\text{CO}_2 \text{ at } T_{\text{mean}} = (p\text{CO}_2)_{\text{obs}} \times \exp[0.0423(T_{\text{mean}} - T_{\text{obs}})]$$

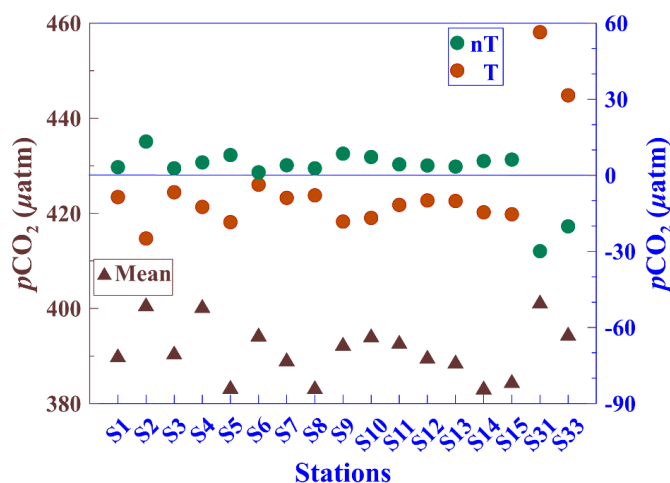
324 $p\text{CO}_2$ at T_{obs} is calculated using the average $p\text{CO}_2$ to determine the $p\text{CO}_2$ value at a
325 given temperature; $p\text{CO}_2$ at T_{mean} is the standardized $p\text{CO}_2$ value at the average
326 temperature; and T_{mean} and T_{obs} are the annual average temperature and the measured
327 temperature on-site, respectively. To assess the impact of temperature (T) and non-
328 temperature (nT) effects on $p\text{CO}_2$, the following equations were employed:



329 T effect = $p\text{CO}_2$ at T_{obs} - $p\text{CO}_2$ at T_{mean}

330 nT effect = $p\text{CO}_2 - p\text{CO}_2$ at T_{obs}

331 The fluctuations in the mean $p\text{CO}_2$ at each monitoring station over time suggest that
332 temperature and non-temperature effects had distinct influences on the average $p\text{CO}_2$
333 at each station (Fig. 7). This means that seasonal changes in $p\text{CO}_2$ are influenced by
334 both temperature and non-temperature effects (e.g., gas exchange, tides, currents,
335 river discharge, upwelling, vertical mixing, and biological processes), with some
336 stations showing larger changes than others. It is believed that the stations with larger
337 $p\text{CO}_2$ variations are likely dominated by either temperature or non-temperature

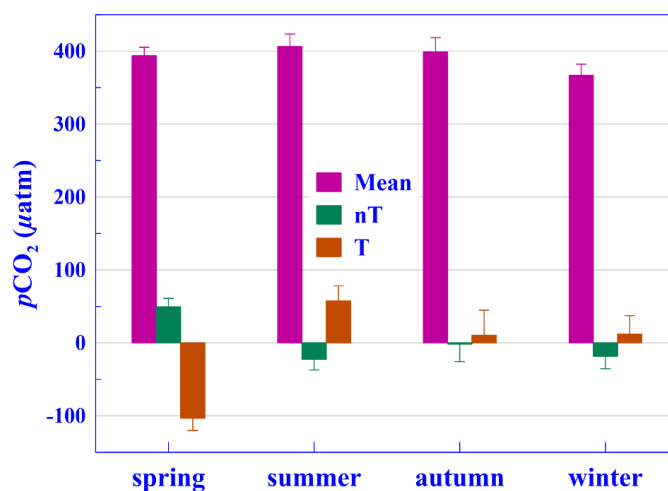


338
339 Fig. 7. Mean values and impact levels of surface water $p\text{CO}_2$ at each station in
340 Nanwan Bay are presented. The "Mean" represents the average value for each
341 station across the four seasons and is plotted on the left y-axis. The terms "nT"
342 and "T" refer to the non-temperature and temperature effects on surface water
343 $p\text{CO}_2$, respectively, and are displayed on the right y-axis for clarity.



344 effects, while the smaller changes reflect the mutual offsetting of the two effects (Dai
345 et al., 2009). For example, the variability in $p\text{CO}_2$ observed at S31 and S33, which are
346 located near the Nuclear Power Plant outlet, is likely driven by temperature change, as
347 the water temperature in this area was consistently higher and exhibited greater
348 variability compared to the surrounding area throughout the year. In fact, we expected
349 that temperature effects on $p\text{CO}_2$ would be more pronounced at these sites.

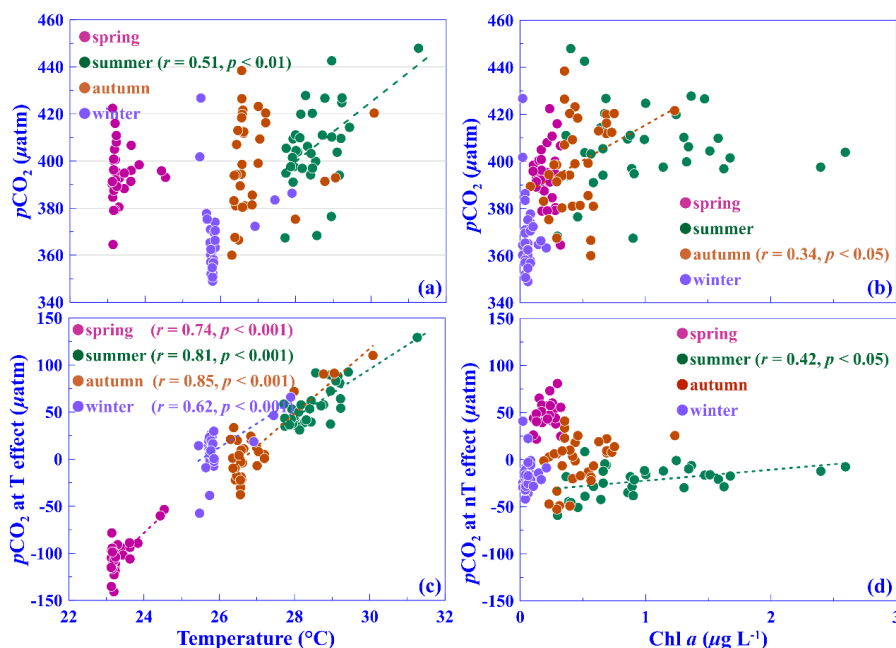
350 During the entire study duration, variation in surface water $p\text{CO}_2$ in Nanwan
351 Bay was influenced by a combination of temperature and non-temperature factors
352 throughout all seasons, albeit with varying degrees of influence in different seasons.



353
354 **Fig. 8.** Mean values and impact levels of surface water $p\text{CO}_2$ in Nanwan Bay during
355 different seasons. "Mean" represents the average value across sampling stations
356 for each season. "nT" denotes non-temperature effects on surface water $p\text{CO}_2$,
357 while "T" signifies temperature effects on surface water $p\text{CO}_2$. Error bars
358 represent standard deviation.



359 Notably, the effect of temperature was more prominent in the spring and summer (Fig.
 360 8). The relationship between surface water $p\text{CO}_2$, surface water temperature, and Chl
 361 a concentration revealed a significant correlation with $p\text{CO}_2$ and temperature in the
 362 summer ($p < 0.01$; Fig. 9a), and a positive correlation between $p\text{CO}_2$ and Chl a in
 363 autumn ($p < 0.05$; Fig. 9b). This suggests that temperature and Chl a may be the factors
 364 affecting surface water $p\text{CO}_2$ in summer and autumn, respectively. In general, Chl a
 365 affects $p\text{CO}_2$ by driving photosynthesis, which removes CO_2 from seawater via



366 **Fig. 9.** Relationships between surface water $p\text{CO}_2$ and (a) temperature, and (b) Chl a ,
 367 (c) the temperature (T) effect on surface water $p\text{CO}_2$ and temperature, and (d)
 368 the non-temperature (nT) effect on surface water $p\text{CO}_2$ and Chl a across
 369 different seasons in Nanwan Bay. The linear relationships, along with the
 370 corresponding r and p values, are provided for reference.
 371



372 phytoplankton activity (Chen et al., 2019). Higher chlorophyll levels suggest
373 increased primary productivity, leading to greater CO₂ drawdowns during the day.

374 To further assess the influence of T and nT effects on surface water *p*CO₂ across

375 different seasons, we compared T-driven surface water *p*CO₂ with temperature and

376 nT-driven surface water *p*CO₂ with Chl *a* (one of the nT factors; Fig. 9c, d).

377 Significant correlations were observed between T-driven surface water *p*CO₂ and

378 temperature in all seasons (Fig. 9c), and between nT-driven surface water *p*CO₂ and

379 Chl *a* during summer (Fig. 9d). Overall, the results (Figs. 8 and 9) indicate that

380 temperature is the primary driver of seasonal *p*CO₂ variation, with non-temperature

381 factors, particularly Chl *a*, also contributing. However, the lower *r* values suggest that

382 additional, unmeasured factors may be influencing the temporal variation in *p*CO₂

383 (Fig. 9d).

384 As mentioned above, seawater *p*CO₂ levels can be influenced by phytoplankton

385 via photosynthesis. Therefore, nutrient availability in seawater primarily affects *p*CO₂

386 levels by either promoting or limiting phytoplankton growth and consequently

387 primary production. In the case of Nanwan Bay, like many coral reef ecosystems, its

388 benthic environment supports nutrient regeneration through processes such as organic

389 carbon decomposition and other processes. However, due to the high shallow water

390 temperature and frequent stratification, regenerative nutrients cannot easily be



391 transported to the shallows. This results in the shallow areas rarely becoming
392 eutrophic (Leichter et al., 1996; Torr ton, 1999; Wolanski and Pickard, 1983).
393 Another reason for Nanwan Bay's oligotrophy is that when nutrients flow into reef
394 areas, resident organisms may quickly utilize them (Wilkerson and Trench, 1986).
395 Although nutrient input from outside the bay is greater than the outward flux, rapid
396 circulation of water in Nanwan Bay leads to unused nutrients being swiftly exported
397 out of the bay (Su, 2009). This causes oligotrophy and high benthic productivity in the
398 area. Su (2009) reported that during spring tides, the water can be replaced in just 1.6
399 tidal cycles. Therefore, nutrient levels and Chl *a* may have only small influences on
400 $p\text{CO}_2$ in Nanwan Bay, with temperature changes and seawater movement having a
401 more significant impact.

402 **3.3 Spatial and temporal variations of $\Delta p\text{CO}_2$ and CO_2 air-sea flux.** The
403 partial pressure difference between CO_2 in surface seawater and the atmosphere,
404 denoted as $\Delta p\text{CO}_2$, indicates the direction of air-sea CO_2 exchange. When $\Delta p\text{CO}_2 > 0$,
405 CO_2 in seawater is released into the atmosphere, contributing to an increase in
406 atmospheric CO_2 concentration (i.e., a source). On the other hand, when $\Delta p\text{CO}_2 < 0$,
407 CO_2 from the atmosphere enters the seawater, acting as a sink for atmospheric CO_2 . In
408 spring, the $\Delta p\text{CO}_2$ range was between -14.3 and $27.7 \mu\text{atm}$, with an average of 7.7
409 $(\pm 10.8) \mu\text{atm}$ (Fig. 10a). The highest value was observed near the Nuclear Power

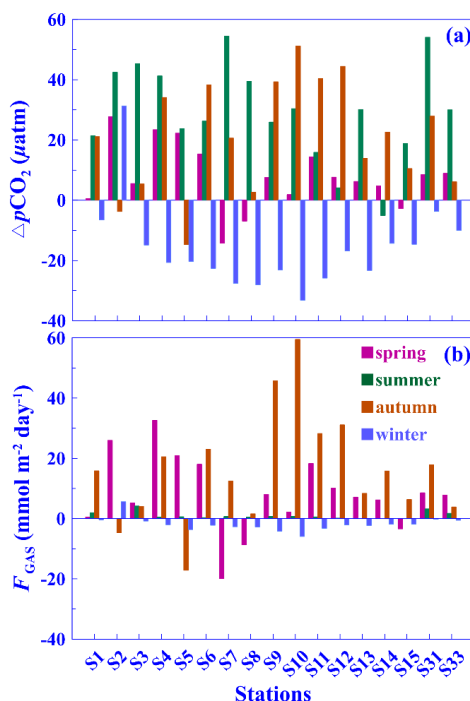


410 Plant outlet station, i.e., St. 2. In summer, it ranged between -5.1 and 54.5 μatm , with
411 an average of 29.3 (± 16.1) μatm . The highest value was measured near station S7. In
412 autumn, the range was between -14.6 and 51.2 μatm , with an average of 21.2 (± 18.6)
413 μatm . The highest value was observed near stations S10-S12. In winter, the range was
414 between -33.2 and 31.3 μatm , with an average of -16.1 (± 14.5) μatm . The highest
415 value occurred near stations S2. It is important to note that $p\text{CO}_2$ measurements in this
416 study were limited to daytime, when photosynthesis is actively occurring, typically
417 resulting in lower $p\text{CO}_2$ levels. As reported in this study and other coral reef
418 ecosystems (Yan et al., 2018), significant diurnal variations in seawater $p\text{CO}_2$ have
419 been observed. Therefore, it is likely that the $\Delta p\text{CO}_2$ values presented here may be
420 underestimates due to this limitation.

421 Based on data from the Central Weather Bureau's Oluanpi buoy, the average
422 sampling date wind speed during the southwest monsoon season (summer) was 1.4
423 (± 1.0) m s^{-1} , while during the northeast monsoon seasons (spring, autumn, & winter),
424 it was 10.6 (± 0.8), 9.2 (± 2.5), and 3.3 (± 0.7) m s^{-1} , respectively. In other words, high
425 wind speeds are consistently observed during the northeast monsoon, in contrast to
426 the relatively lower wind speeds experienced during the summer season along the
427 coast of Taiwan (Ren et al., 2022). Utilizing these wind speed values, the CO_2 air-sea
428 exchange flux in Nanwan Bay was calculated (Figure 10b). During spring, the CO_2



429 flux ranged from -19.9 to 32.6 mmol m⁻² day⁻¹ (average=8.2±12.7 mmol m⁻² day⁻¹). In
 430 summer, the CO₂ flux ranged from 0.0 to 4.2 mmol m⁻² day⁻¹ (average=0.9±1.2 mmol
 431 m⁻² day⁻¹). During autumn, the CO₂ flux ranged from -17.1 to 59.5 mmol m⁻² day⁻¹,
 432 with an average of 16.0±18.4 mmol m⁻² day⁻¹. Finally, in winter, the CO₂ flux ranged
 433 from -5.9 to 5.6 mmol m⁻² day⁻¹, with an average of -1.8±2.4 mmol m⁻² day⁻¹. These
 434 findings highlight that wind speed plays a crucial factor in regulating CO₂ air-sea
 435 exchange flux. Moreover, any factors that impact wind speed can significantly affect
 436 gas exchange estimates. For instance, when using daily wind speed data for the



437
 438 **Fig. 10.** Seasonal variation in (a) surface water $\Delta p\text{CO}_2$ and (b) air-sea CO₂ exchange
 439 flux (F_{GAS}) at each station. Values are presented relative to the annual mean
 440 (scaled to 0).



441 sampling month, the CO₂ flux increase from 0.9 (±1.2) to 12.4 (±9.9) mmol m⁻² day⁻¹
442 in summer, and 16.0 (±18.4) to 29.5 (±11.9) mmol m⁻² day⁻¹ in fall (Table S2).

443 The area between Cape Moubitou and Cape Oluanpi, covering approximately 30
444 km² (Fig. 1), shows CO₂ fluxes of 6.2 tC, 0.7 tC, 11.9 tC, and -1.3 tC in spring,
445 summer, fall, and winter, respectively, based on wind speeds recorded on the sampling
446 date (Table S2). However, when using daily wind speed data for the sampling month,
447 significant changes in CO₂ flux are observed, such as an increase from 0.7 to 9.4 tC in
448 summer and from 11.9 to 21.9 tC in fall (Table S2). This indicates that CO₂ flux
449 estimates are highly sensitive to wind speed variability, introducing uncertainty in
450 determining whether Nanwan Bay's coral reef ecosystem functions as a carbon sink or
451 source based on this limited dataset. Most coral reef areas act as atmospheric CO₂
452 sources, such as Bermuda (14.4 gC m⁻² year⁻¹; Bates et al., 2001), Okinawa (21.6 gC
453 m⁻² year⁻¹; Ohde and Van Woesik, 1999), the Great Barrier Reef (18 gC m⁻² year⁻¹;
454 Frankignoulle et al., 1996), French Polynesia (1.2 gC m⁻² year⁻¹; Frankignoulle et al.,
455 1996; Gattuso et al., 1997; Gattuso et al., 1993), and Hawaii (17.4 gC m⁻² year⁻¹;
456 Fagan and Mackenzie, 2007). In addition to wind speed, the primary factor
457 influencing the atmospheric carbon sink/source nature of this coral reef ecosystem is
458 the substantial vertical mixing and upwelling observed during the spring and winter.
459 These periods are characterized by a well-mixed water column, lower seawater



460 temperatures, and reduced $p\text{CO}_2$ levels, particularly during the northeast monsoon,
461 when high winds significantly enhance the CO_2 sea-air gas exchange flux. In contrast,
462 despite high $\Delta p\text{CO}_2$ values in summer, wind speeds were relatively low, especially
463 during the southwest monsoon, making the CO_2 sea-air flux insufficient to offset the
464 carbon sink observed in winter. Although land-based inputs can affect nearshore
465 environments, leading to $p\text{CO}_2$ variations and influencing CO_2 sea-air flux (Meng et
466 al., 2008; De Carlo et al., 2007), the impact here is minimal, as no large river is near
467 this coral reef ecosystem. Additionally, the wind speed data used for CO_2 flux
468 calculations were collected from buoys within the ecosystem, providing an accurate
469 reflection of local conditions. It is important to note that short-term and long-term
470 wind speed fluctuations, prevailing climate conditions, and specific events can affect
471 CO_2 flux calculations, given the nonlinear relationship between wind speed and gas
472 exchange (Chou et al., 2011; Evans et al., 2012; De La Paz et al., 2011).

473 **4. Conclusions**

474 Nanwan Bay experiences notable seasonal variations in temperature and salinity,
475 largely influenced by the South China Sea and the Kuroshio Current. These changes
476 impact the seawater carbonate system (including $p\text{CO}_2$), with additional influences
477 from vertical water movement and biological activity. Temperature emerged as the
478 primary driver of spatio-temporal variations in $p\text{CO}_2$, particularly at the consistently



479 warmer outlet station. Non-temperature factors also played a role during the spring,
480 while the interaction between temperature and other factors became more prominent
481 in the autumn and winter. During the winter, the bay absorbs more CO₂ from the
482 atmosphere, whereas in the spring, summer, and autumn, it releases more CO₂ than it
483 absorbs. The complex interplay of temperature, water mass origin, vertical water
484 movement, and biological activity in Nanwan Bay significantly affects its carbon
485 dioxide dynamics and its influence on atmospheric CO₂ levels.

486 **5. Acknowledgements**

487 This study was supported by grants from the Ministry of Science and Technology
488 of Taiwan (MOST) and National Science and Technology Council (NSTC) of Taiwan
489 through various grants, specifically: MOST 111-2611-M-259-002, MOST 110-2611-
490 M-259-002, MOST 109-2611-M-259-003, MOST 108-2611-M-291-005, MOST 107-
491 2611-M-291-001, and MOST 106-2611-M-291-006 awarded to PJM. CCC was also
492 supported by NSTC 112-2611-M-003-004. and NSTC 113-2611-M-003-002.
493 Data were submitted to Dryad for archiving (doi: 10.5061/dryad.63xsj3v7d).

494 **6. Credit author statement**

495 This manuscript was conceptualized by PJM and CCC; CMC and HYH conducted
496 investigations on all cruises and collected and analyzed the initial data; PJM, ABM,



497 and CCC wrote the initial draft; all authors provided comments and edits. The authors

498 declare that they have no competing interests.



499

References

- 500 Albright, R., Caldeira, L., Hosfelt, J., Kwiatkowski, L., Maclaren, J. K., Mason, B.
501 M., Nebuchina, Y., Ninokawa, A., Pongratz, J., Ricke, K. L., Rivlin, T.,
502 Schneider, K., Sesboüé, M., Shamberger, K., Silverman, J., Wolfe, K., Zhu, K.,
503 and Caldeira, K.: Reversal of ocean acidification enhances net coral reef
504 calcification, *Nature*, 531, 362-365, 10.1038/nature17155, 2016.
- 505 Bates, N. R., Samuels, L., and Merlivat, L.: Biogeochemical and physical factors
506 influencing seawater $f\text{CO}_2$ and air-sea CO_2 exchange on the Bermuda coral reef,
507 *Limnol. Oceanogr.*, 46, 833-846, 10.4319/lo.2001.46.4.0833, 2001.
- 508 Borges, A. V. and Frankignoulle, M.: Distribution of surface carbon dioxide and air-
509 sea exchange in the upwelling system off the Galician coast, *Glob. Biogeochem.*
510 *Cycles*, 16, 1020, 10.1029/2000GB001385, 2002.
- 511 Borges, A. V., Delille, B., and Frankignoulle, M.: Budgeting sinks and sources of CO_2
512 in the coastal ocean: Diversity of ecosystems counts, *Geophys. Res. Lett.*, 32,
513 n/a-n/a, 10.1029/2005gl023053, 2005.
- 514 Cai, W. J., Wang, Z. A., and Wang, Y.: The role of marsh-dominated heterotrophic
515 continental margins in transport of CO_2 between the atmosphere, the land-sea
516 interface and the ocean., *Geophys. Res. Lett.*, 30, 1849,
517 10.1029/2003GL017633, 2003.
- 518 Chen, C.-C., Chou, W.-C., Hung, C.-C., and Gong, G.-C.: Nutrient sources,
519 phytoplankton blooms, and hypoxia along the Chinese coast in the East China
520 Sea: Insight from summer 2014, *Mar. Pollut. Bull.*, 205, 116692,
521 10.1016/j.marpolbul.2024.116692, 2024.
- 522 Chen, C.-C., Hsieh, H.-Y., Mayfield, A. B., Chang, C.-M., Wang, J.-T., and Meng, P.-
523 J.: The Key impact on water quality of coral reefs in Kenting National Park, M.
524 *Mar. Sci. Eng.*, 10, 207, 10.3390/jmse10020270, 2022.
- 525 Chen, C.-C., Shiah, F. K., Lee, H. J., Li, K. Y., Meng, P. J., Kao, S. J., Tseng, Y. F.,
526 and Chung, C. L.: Phytoplankton and bacterioplankton biomass, production and
527 turnover in a semi-enclosed embayment with spring tide induced upwelling,
528 *Mar. Ecol. Prog. Ser.*, 304, 91-100, 10.3354/meps304091, 2005.
- 529 Chen, C. T. A., Hsing, L. Y., Liu, C. L., and Wang, S. L.: Degree of nutrient
530 consumption of upwelled water in the Taiwan Strait based on dissolved organic
531 phosphorus or nitrogen, *Mar. Chem.*, 87, 73-86,
532 10.1016/j.marchem.2004.01.006, 2004.
- 533 Chen, S., Hu, C., Barnes, B. B., Wanninkhof, R., Cai, W.-J., Barbero, L., and Pierrot,
534 D.: A machine learning approach to estimate surface ocean $p\text{CO}_2$ from satellite
535 measurements, *Remote Sens Environ.*, 228, 203-226, 10.1016/j.rse.2019.04.019,



- 536 2019.
- 537 Chou, W. C., Gong, G. C., Tseng, C. M., Sheu, D. D., Hung, C. C., Chang, L. P., and
538 Wang, L. W.: The carbonate system in the East China Sea in winter, *Mar.*
539 *Chem.*, 123, 44-55, 10.1016/j.marchem.2010.09.004, 2011.
- 540 Dai, M. H., Lu, Z. M., Zhai, W. D., Chen, B. S., Cao, Z. M., Zhou, K. B., Cai, W. J.,
541 and Chen, C. T. A.: Diurnal variations of surface seawater $p\text{CO}_2$ in contrasting
542 coastal environments, *Limnol. Oceanogr.*, 54, 735-745,
543 10.4319/lo.2009.54.3.0735, 2009.
- 544 De Carlo, E. H., Hoover, D. J., Young, C. W., Scheinberg, R. D., and Mackenzie, F. T.:
545 Impact of storm runoff from tropical watersheds on coastal water quality and
546 productivity, *Appl Geochem*, 22, 1777-1797,
547 10.1016/j.apgeochem.2007.03.034, 2007.
- 548 de la Paz, M., Huertas, E. M., Padín, X.-A., González-Dávila, M., Santana-Casiano,
549 M., Forja, J. M., Orbi, A., Pérez, F. F., and Ríos, A. F.: Reconstruction of the
550 seasonal cycle of air-sea CO_2 fluxes in the Strait of Gibraltar, *Mar. Chem.*, 126,
551 155-162, 10.1016/j.marchem.2011.05.004, 2011.
- 552 Dickson, A. G. and Millero, F. J.: A comparison of the equilibrium constants for the
553 dissociation of carbonic acid in seawater media, *Deep-Sea Res. I*, 34, 1733-
554 1743, 10.1016/0198-0149(87)90021-5, 1987.
- 555 Dugdale, R. C. and Wilkerson, F. P.: New production in the upwelling central at Point
556 Conception, California: temporal and spatial patterns, *Deep-Sea Res. I*, 36, 985-
557 1007, 1989.
- 558 Evans, W., Hales, B., Strutton, P. G., and Ianson, D.: Sea-air CO_2 fluxes in the western
559 Canadian coastal ocean, *Progress in Oceanography* 101, 78-91,
560 10.1016/j.pocean.2012.01.003, 2012.
- 561 Fabry, V. J., Seibel, B. A., Feely, R. A., and Orr, J. C.: Impacts of ocean acidification
562 on marine fauna and ecosystem processes, *ICES Journal of Marine Science*, 65,
563 414-432, 10.1093/icesjms/fsn048, 2008.
- 564 Fagan, K. E. and Mackenzie, F. T.: Air-sea CO_2 exchange in a subtropical estuarine-
565 coral reef system, Kaneohe Bay, Oahu, Hawaii, *Mar. Chem.*, 106, 174-191,
566 10.1016/j.marchem.2007.01.01, 2007.
- 567 Fay, A. R., Gregor, L., Landschützer, P., McKinley, G. A., Gruber, N., Gehlen, M.,
568 Iida, Y., Laruelle, G. G., Rödenbeck, C., Roobaert, A., and Zeng, J.: SeaFlux:
569 harmonization of air-sea CO_2 fluxes from surface $p\text{CO}_2$ data products using a
570 standardized approach, *Earth Syst. Sci. Data.*, 13, 4693-4710, 10.5194/essd-13-
571 4693-2021, 2021.
- 572 Frankignoulle, M., Copin-Montegut, G., Pichon, M., Gattuso, J. P., Biondo, R., and
573 Bourge, I.: Carbon fluxes in coral reefs. II. Eulerian study of inorganic carbon



- 574 dynamics and measurement of air-sea CO₂ exchanges, *Marine Ecology.*
575 *Progress Series*, 145, 123-132, 10.3354/meps145123, 1996.
- 576 Frankignoulle, M., Abril, G., Borges, A., Bourge, I. I., Canon, C., Delille, B., Libert,
577 E., and Theate, J. M.: Carbon dioxide emission from european estuaries,
578 *Science*, 282, 434-436, 1998.
- 579 Friederich, G. E., Walz, P. M., Burczynski, M. G., and Chavez, F. P.: Inorganic carbon
580 in the central California upwelling system during the 1997–1999 El Niño–La
581 Niña event, *Prog. Oceanogr.*, 54, 185-203, 10.1016/S0079-6611(02)00049-6,
582 2002.
- 583 Gattuso, J.-P., Frankignoulle, M., and Smith, S. V.: Measurement of community
584 metabolism and significance in the coral reef CO₂ source-sink debate, *Proc.*
585 *Natl. Acad. Sci. U. S. A.*, 96, 13017-13022, 10.1073/pnas.96.23.13017, 1999.
- 586 Gattuso, J.-P., Pichon, M., Delesalle, B., and Frankignoulle, M.: Community
587 metabolism and air-sea CO₂ fluxes in a coral-reef ecosystem (Moorea, French-
588 Polynesia), *Mar. Ecol. Prog. Ser.*, 96, 259-267, 10.3354/meps096259, 1993.
- 589 Gattuso, J.-P., Payri, C. E., Pichon, M., Delesalle, B., and Frankignoulle, M.: Primary
590 production, calcification, and air-sea CO₂ fluxes of a macroalgal-dominated
591 coral reef community (Moorea, French Polynesia), *J. Phycol.*, 33, 729-738,
592 10.1111/j.0022-3646.1997.00729.x 1997.
- 593 Goyet, C., Eiseheid, G., McCue, S. J., Bellerby, R. G. J., Millero, F. J., and
594 O'Sullivan, D. W.: Temporal variations of pCO₂ in surface seawater of the
595 Arabian Sea in 1995, *Deep-Sea Research I, Oceanographic Research*, 45, 609-
596 623, 10.1016/S0967-0637(97)00085-X 1998.
- 597 Gran, G.: Determination of the equivalence point in potentiometric titrations. Part II,
598 *Analyst*, 77, 661-671, 10.1039/an9527700661, 1952.
- 599 Hales, B., Takahashi, T., and Bandstra, L.: Atmospheric CO₂ uptake by a coastal
600 upwelling system, *Glob. Biogeochem. Cycles*, 19, GB1009,
601 10.1029/2004GB002295,, 2005.
- 602 Ibanhez, J. S. P., Diverres, D., Araujo, M., and Lefevre, N.: Seasonal and interannual
603 variability of sea-air CO₂ fluxes in the tropical Atlantic affected by the Amazon
604 River plume, *Glob. Biogeochem. Cycles*, 29, 1640-1655,
605 10.1002/2015gb005110, 2015.
- 606 IPCC: Summary for policymakers, Cambridge, United Kingdom and New York, NY,
607 USA, 3-32, 10.1017/9781009157896, 2021.
- 608 Ito, R. G., Schneider, B., and Thomas, H.: Distribution of surface *f*CO₂ and air-sea
609 fluxes in the Southwestern subtropical Atlantic and adjacent continental shelf, *J.*
610 *Mar. Syst.*, 56, 227-242, 10.1016/j.jmarsys.2005.02.005, 2005.
- 611 Kayanne, H., Suzuka, A., and Saito, H.: Diurnal changes in the partial pressure of



- 612 carbon dioxide in coral reef water, *Science*, 269, 214-216,
613 10.1126/science.269.5221.214, 1995.
- 614 Lee, H.-J., Chao, S.-Y., and Fan, K.-L.: Flood-Ebb disparity of tidally induced re-
615 circulation eddies in a semi-enclosed basin: Nan Wan Bay, *Cont. Shelf Res.*, 19,
616 871-890, 10.1016/S0278-4343(99)00006-0, 1999a.
- 617 Lee, H.-J., Chao, S.-Y., Fan, K.-L., and Kuo, T.-Y.: Tide-induced eddies and
618 upwelling in a semi-enclosed basin: Nan Wan, *Estuar. Coast. Shelf Sci.*, 49,
619 775-787, 10.1006/ecss.1999.0524, 1999b.
- 620 Lee, H.-J., Chao, S.-Y., Fan, J.-L., Wnag, Y.-H., and Liang, N.-J.: Tidally induced
621 upwelling in a semi-enclosed basin: Nan Wan Bay, *J. Oceanogr.*, 53, 467-480,
622 1997.
- 623 Lee, H. J.: Tidally induced eddies and cold water intrusion in Nan Wan Bay, PhD
624 dissertation, Institute of Oceanography, National Taiwan University, Taipei,
625 Taiwan, Taipei, Taiwan, 127 pp., 1999.
- 626 Leichter, J. J., Wing, S. R., Miller, S. L., and Denny, M. W.: Pulsed delivery of
627 subthermocline water to Conch Reef (Florida Keys) by internal tidal bores,
628 *Limnol. Oceanogr.*, 41, 1490-1501, 10.4319/lo.1996.41.7.1490, 1996.
- 629 Lewis, E. and Wallace, D. W. R.: Program developed for CO₂ system calculations,
630 Carbon Dioxide Information Analysis Center, Oak Ridge National Laboratory,
631 Oak Rيدةge, TN, USARep. ORNL/CDIAC-105, 10.2172/639712, 1998.
- 632 Liang, W. D., Yang, Y. J., Tang, T. Y., and Chuang, W. S.: Kuroshio in the Luzon
633 Strait, *J. Geophys. Res. Oceans*, 113, Artn C08048, 10.1029/2007jc004609,
634 2008.
- 635 Lønborg, C., Calleja, M. L., Fabricius, K. E., Smith, J. N., and c, E. P. A.: The Great
636 Barrier Reef: a source of CO₂ to the atmosphere, *Mar. Chem.*, 210, 24-33,
637 10.1016/j.marchem.2019.02.003, 2019.
- 638 Mayer, B., Rixen, T., and Pohlmann, T.: The spatial and temporal variability of air-sea
639 CO₂ fluxes and the effect of net coral reef calcification in the Indonesian seas: A
640 numerical sensitivity study, *Frontiers in Marine Science*, 5, 116,
641 10.3389/fmars.2018.00116, 2018.
- 642 Mehrbach, C., Culberson, C. H., Hawley, J. E., and Pytkowicz, R. M.: Measurement
643 of apparent dissociation constants of carbonic-acid in seawater at atmospheric
644 pressure, *Limnol. Oceanogr.*, 18, 897-907, 10.4319/lo.1973.18.6.0897, 1973.
- 645 Meng, P. J., Lee, H. J., Wang, J. T., Chen, C. C., Lin, H. J., Tew, K. S., and Hsieh, W.
646 J.: A long-term survey on anthropogenic impacts to the water quality of coral
647 reefs, southern Taiwan, *Environmental Pollution*, 156, 67-75,
648 10.1016/j.envpol.2007.12.039, 2008.
- 649 Meng, P. J., Chung, K. N., Chen, J. P., Chen, M. H., Liu, M. C., Chang, Y. C., Fan, T.



- 650 Y., Lin, H. J., Liu, B. R., Chang, C. M., Fang, L. S., and Shao, K. T.: Long-term
651 ecological monitoring and studies of human activities on the marine ecosystem
652 of Kenting National Park. (in Chinese with English abstract), 17, 89–111, 2007.
- 653 Murray, J. W., Johnson, E., and Garside, C.: A U.S. JGOFS Process Study in the
654 equatorial Pacific (EqPac): Introduction, Deep-Sea Res. II Top. Stud. Oceanogr.,
655 42, 275-293, 10.1016/0967-0645(95)00044-Q, 1995.
- 656 Nan, F., Xue, H., and Yu, F.: Kuroshio intrusion into the South China Sea: A review,
657 Prog. Oceanogr., 137, 314-333, 10.1016/j.pocean.2014.05.012, 2015.
- 658 Ohde, S. and Van Woesik, R.: Carbon dioxide flux and metabolic processes of a coral
659 reef, Okinawa, Bull. Mar. Sci., 65, 559-576, 1999.
- 660 Parsons, T. R., Maita, Y., and Lalli, C. M.: A manual of chemical and biological
661 methods for seawater analysis, Pergamon Press, New York, 173 pp.,
662 10.1016/C2009-0-07774-5, 1984.
- 663 Ren, L., Ji, J., Wang, Y., Bu, S., Lu, Z., and Luo, X.: Investigation into spatiotemporal
664 characteristics of coastal winds around the Taiwan Island, Energy Rep., 8, 419-
665 427, 10.1016/j.egy.2022.03.108, 2022.
- 666 Ries, J. B.: A physicochemical framework for interpreting the biological calcification
667 response to CO₂-induced ocean acidification, Geochim. Cosmochim. Acta, 75,
668 4053-4064, 10.1016/j.gca.2011.04.025, 2011.
- 669 Schimel, D. S., House, J. I., Hibbard, K. A., Bousquet, P., Ciais, P., Peylin, P.,
670 Braswell, B. H., Apps, M. J., Baker, D., Bondeau, A., Canadell, J., Churkina, G.,
671 Cramer, W., Denning, A. S., Field, C. B., Friedlingstein, P., Goodale, C.,
672 Heimann, M., Houghton, R. A., Melillo, J. M., III, B. M., Murdiyarso, D.,
673 Noble, I., Pacala, S. W., Prentice, I. C., Raupach, M. R., Rayner, P. J., Scholes,
674 R. J., Steffen, W. L., and Wirth, C.: Recent patterns and mechanisms of carbon
675 exchange by terrestrial ecosystems, Nature, 414, 169-172, 10.1038/35102500,
676 2001.
- 677 Sitch, S., Friedlingstein, P., Gruber, N., Jones, S. D., Murray-Tortarolo, G., Ahlström,
678 A., Doney, S. C., Graven, H., Heinze, C., Huntingford, C., Levis, S., Levy, P. E.,
679 Lomas, M., Poulter, B., Viovy, N., Zaehle, S., Zeng, N., Arneeth, A., Bonan, G.,
680 Bopp, L., Canadell, J. G., Chevallier, F., Ciais, P., Ellis, R., Gloor, M., Peylin, P.,
681 Piao, S. L., Le Quéré, C., Smith, B., Zhu, Z., and Myneni, R.: Recent trends and
682 drivers of regional sources and sinks of carbon dioxide, Biogeosciences, 12,
683 653-679, 10.5194/bg-12-653-2015, 2015.
- 684 Su, C.-H.: The study of the nutrient flux in Nan-Wan Bay, National Taiwan Ocean
685 University, National Taiwan ocean university, 101 pp., 2009.
- 686 Suzuki, A.: Combined effects of photosynthesis and calcification on the partial
687 pressure of carbon dioxide in seawater, J. Oceanogr., 54, 1-7,



- 688 10.1007/BF02744376, 1998.
- 689 Suzuki, A. and Kawahata, H.: Reef water CO₂ system and carbon production of coral
690 reefs: Topographic control of system-level performance, in: Global
691 environmental change in the ocean and on land, edited by: Shiyomi, M.,
692 Kawahata, H., Koizumi, H., Tsuda, A., and Awaya, Y., TERRAPUB, 229-248,
693 2004.
- 694 Takahashi, T., Sutherland, S. C., Sweeney, C., Poisson, A., Metzl, N., Tilbrook, B.,
695 Bates, N., Wanninkhof, R., Feely, R. A., Sabine, C., Olafsson, J., and Nojiri, Y.:
696 Global sea-air CO₂ flux based on climatological surface ocean pCO₂, and
697 seasonal biological and temperature effects, Deep-Sea Res. II Top. Stud.
698 Oceanogr., 49, 1601-1622, 10.1016/S0967-0645(02)00003-6, 2002.
- 699 Tew, K. S., Leu, M. Y., Wang, J. T., Chang, C. M., Chen, C. C., and Meng, P. J.: A
700 continuous, real-time water quality monitoring system for the coral reef
701 ecosystems of Nanwan Bay, Southern Taiwan, Mar. Pollut. Bull., 85, 641-647,
702 10.1016/j.marpolbul.2013.11.022, 2014.
- 703 Torréton, J.-P.: Biomass, production and heterotrophic activity of bacterioplankton in
704 the Great Astrolabe Reef lagoon (Fiji), Coral Reefs, 18, 43-53,
705 10.1007/s003380050152, 1999.
- 706 Wang, Z. A. and Cai, W. J.: Carbon dioxide degassing and inorganic carbon export
707 from a marsh-dominated estuary (the Duplin River): a marsh CO₂ pump,
708 Limnol. Oceanogr., 49, 341-354, 10.4319/lo.2004.49.2.0341, 2004.
- 709 Wanninkhof, R.: Relationship between wind speed and gas exchange over the ocean,
710 J. Geophys. Res., 97, 7373-7382, 10.1029/92JC00188, 1992.
- 711 Ware, J. R., Smith, S. V., and Reaka-Kudla, M. L.: Coral reefs: sources or sinks of
712 atmospheric CO₂?, Coral Reefs, 11, 127-130, 10.1007/BF00255465, 1992.
- 713 Watanabe, A. and Nakamura, T.: Carbon dynamics in coral reefs, in: Blue Carbon in
714 Shallow Coastal Ecosystems: carbon dynamic, policy, and implementation,
715 edited by: Kuwae, T., and Hori, M., Springer, Singapore, 273-293, 10.1007/978-
716 981-13-1295-3, 2019.
- 717 Weiss, R. F.: Carbon dioxide in water and seawater: the solubility of a non-ideal gas,
718 Mar. Chem., 2, 203-215, 10.1016/0304-4203(74)90015-2, 1974.
- 719 Wilkerson, F. P. and Trench, R. K.: Uptake of dissolved inorganic nitrogen by the
720 symbiotic clam *Tridacna gigas* and the coral *Acropora* sp., Mar. Biol., 93, 237-
721 246, 10.1007/BF00508261, 1986.
- 722 Wolanski, E. and Pickard, G. L.: Upwelling by internal tides and Kelvin waves at the
723 continental shelf break on the Great Barrier Reef, Australian Journal of Marine
724 and Freshwater Research, 34, 65-80, 10.1071/MF9830065, 1983.
- 725 Yan, H., Yu, K., Shi, Q., Lin, Z., Zhao, M., Tao, S., Liu, G., and Zhang, H.: Air-sea



- 726 CO₂ fluxes and spatial distribution of seawater pCO₂ in Yongle Atoll, northern-
727 central South China Sea, *Cont. Shelf Res.*, 165, 71-77,
728 10.1016/j.csr.2018.06.008, 2018.
- 729 Yan, H. Q., Yu, K. F., Shi, Q., Tan, Y. H., Zhang, H. L., Zhao, M. X., Li, S., Chen, T.
730 R., Huang, Y., and Wang, P. X.: Coral reef ecosystems in the South China Sea as
731 a source of atmospheric CO₂ in summer, *Chin. Sci. Bull.*, 56, 676-684,
732 10.1007/s11434-011-4372-8, 2011.
- 733 Yang, R. T. and Dai, C. F.: Community structure and species diversity of reef corals at
734 Nanwan Bay, Taiwan, *Acta Oceanogr. Taiwanica*, 11, 238-251, 1980.
- 735 Yuan, D., Han, W., and Hu, D.: Surface Kuroshio path in the Luzon Strait area derived
736 from satellite remote sensing data, *J. Geophys. Res.*, 111, C11007,
737 10.1029/2005JC003412, 2006.
- 738